KASDI MERBAH UNIVERSITY - OUARGLA
Faculty of Applied Sciences
Department of electrical engineering

FINAL STUDY DISSERTATION
In the aim of obtaining MASTER Degree ACADEMIC
Domain: Science and Technology
Option: Electrical engineering
Specialty: Industrial Electrotechnics

Presented by:
BERIALA MOHAMMED MOUNIR KHEMIS ABD ERRAOUF

Theme:

Optimization by simulation of a thin film solar cell based on lead sulphide (PbS)

Publicly debated on: / 06 / 2022 in front of the examining committee composed of:

Mr Louazene Lakhdar	MCA	President	KMU Ouargla
Mr Djafour Ahmed	Professor	Examiner	KMU Ouargla
Mr BenmirAbdelkader	MCB	Supervisor	KMU Ouargla

Academic year: 2021/2022

Dedication

I dedicate this humble work primarily to my father and mother who have given me all the help to reach this stage and achieve all the goals and ambitions that I pursue for all my brothers, from the oldest to the youngest. My sincere greetings to all my family and all my friends, one by one, to everyone who supported me from near or far to complete this note, my thanks and gratitude.To all my teachers from primary school until now to all the teachers of the electrical engineering department

Beriala Mohammed Mounir

Dedication

Praise be to God, the All-Hearing, the All-Knowing, the Possessor of Glory and Great Grace. I thank God first for reaching these crucial moments, the end of my academic career, and the beginning of my academic career.Those whom God has recommended in His Mighty Book.My dear mother and father who lighted my rugged path in the pitch darkness.To the bright twinkling stars in my life, my brothers, my brothers and their spouses, each in his name.Companions in the path, my dear friends, and I will not forget the buds of hope, as they are the adornment of the life of the world.

k.abderraouf

Thanks

We thank God Almighty, who gave us patience, will and determination to complete this graduation thesis.

We extend special thanks to Mr. Benmir Abdelkader (Teacher in the Department of Electrical Engineering, University of Kasdi Merbah - Ouargla) for agreeing to supervise us, and for his constant interest that guided us in our work, and for providing a helping hand and assistance to us and for his advice during this graduation thesis.

We warmly thank the members of the jury for the honor they have shown us by accepting us

To evaluate our work.

Finally, we salute all the teachers and staff of the Faculty of Applied Sciences,

Department of electrical engineering and especially teachers of Industrial Electrotechnics specialty, not forgetting the Electrotechnics master's degree students.

List of Figures

Abstract

The aim of this work is to optimize by simulation, using the SCAPS software, some parameters of the PbS absorber layer of a thin film solar cell. These parameters are the thickness, the bandgap, the doping density and the defect density. The results found showed that the best photovoltaic performances of the solar cell such as: V_{CO} = 0.9979 V, J_{sc} = 31.58 mA/cm^2, FF = 85.70 % and η = 27.01% are obtained for XPbS = 3 µm, Eg = 1.4 eV, $N_A = 10^{16}$ cm^{-3} and $N_t = 10^{10}$ cm^{-3}.

Résumé

L'objectif de ce travail est d'optimiser par simulation, à l'aide du logiciel SCAPS, certains paramètres de la couche absorbante en PbS d'une cellule solaire à couches minces. Ces paramètres sont l'épaisseur, la bande interdite, la densité de dopage et la densité de défauts. Les résultats trouvés ont montré que les meilleures performances photovoltaïques de la cellule solaire telles que : VCO = 0.9979 V, Jsc = 31.58 mA/cm^2, FF = 85.70 % and η = 27.01% sont obtenues pour XPbS = 3 µm, Eg = 1.4 eV, $N_A = 10^{16}$ cm^{-3} and $N_t = 10^{10}$ cm^{-3}.

ملخص

الهدف من هذا العمل هو تحسين بعض معاملات طبقة الامتصاص PbS لخلية شمسية رقيقة عن طريق المحاكاة باستخدام برنامج SCAPS. هذه المعاملات هي السُمك، حزمة الفجوة، كثافة المنشطات وكثافة العيوب. أظهرت النتائج التي تم التوصل إليها أن أفضل أداء للخلية الشمسية على ذكر VCO = 0.9979 V، Jsc = 31.58 mA/cm^2، FF = 85.70 % و η = 27.01% تم الحصول عليها من أجل XPbS = 3 µm، Eg = 1.4 eV، $N_A = 10^{16}$ cm^{-3} و $N_t = 10^{10}$ cm^{-3}.

List of Figures

List of tables

Summary

General Introduction

The Sun, an almost unlimited source of energy, is at the origin of an impressive number of biological effects, which participate directly or indirectly in animal and plant life: it provides heat, allows photosynthesis, vision, conditions biological rhythms, etc.

The originality of photovoltaic energy as it is understood here is to directly transform sunlight into electricity. In addition, when we know that the total solar energy supply on the planet is several thousand times higher than our overall energy consumption, we understand the interest of such an approach. Renewable, this energy respects our environment by reducing greenhouse gas emissions.

Prices continue to fall thanks to the increase in production volumes because the market is strongly stimulated by the purchase of electricity-by-electricity companies. Many photovoltaic cells have emerged to make the best use of sunlight through solar panels.

In order to produce electricity, these solar cells consist of a semi-conductor material, which converts the energy of solar radiation into electricity. Silicon or other semiconductor materials are used, but each technology has strengths and weaknesses in this promising area.

Lead sulfide (PbS) is one of the most suitable semiconductor materials with high absorption coefficient. It has the most favorable bandgap energy and is very stable with low-cost material. Therefore, many researchers have worked to improve the performance of PbS-based thin film solar cells.

Simulation is a very important tool for optimizing the structure and the different parameters of the constituent layers of PV solar cells.

In this work, we will use the SCAPS software to perform the simulation in order to optimize the thickness, the bandgap, the doping density and the defect density of the PbS absorber layer of a thin film solar cells.

This dissertation is organized as follows:

- ✓ In the first chapter, we call on some basic notions in the photovoltaic field.
- ✓ The second chapter is devoted to a more precise study of the Pbs material which is considered as the absorber layer of the PV solar cell.
- ✓ The third chapter is reserved for the optimization of various physical and geometrical parameters of a Pbs-based thin film solar cell. The interpretation of the results obtained gives us the optimal value of each optimized parameter.
- ✓ Finally, we will end this thesis with a general conclusion.

Chapter I

Basic notions on photovoltaic solar cells

I. 1. Introduction

In this chapter, we start with a brief history of photovoltaic solar cells. Next, we will give an overview of solar radiation. After, we will give the definition of PV solar cell, its operating principle, as well as its equivalent diagram and a brief reminder on semiconductor materials. Finally, the different photovoltaic solar cell technologies will be described.

I. 2. History

- In 1839: The French physicist Edmond Becquerel discovered the process of using sunlight to produce electric current in a solid material. This is the photovoltaic effect.
- In 1873: Discovery of the photoconductivity of selenium by Willoughby Smith.
- In 1905: Einstein discovered that the energy of these quanta of light is proportional to the frequency of the electromagnetic wave.
- In 1954: Gerald Pearson, Daryl Chapin and Calvin Fuller, develop a high-efficiency photovoltaic cell at a time when the emerging space industry is looking for new solutions to power its satellites.
- In 1958: A cell with a efficiency of 9 % is developed. The first satellites powered by solar cells are sent into space.

- In 1983: The first car powered by photovoltaic energy travels a distance of 4000 km in Australia.

- In 1995: Grid-connected photovoltaic rooftop programs were launched in Japan and Germany, and have become widespread since 2001 [1,2].

I. 3. Solar radiation

The electromagnetic radiation is made up of "grains" of light called photons. The energy E of each photon is directly related to the wavelength λ by the Equations [3]:

$$E = \frac{h.c}{\lambda} \quad (I.1)$$

Where, h is the Plank's constant given as 6.626×10^{34} Js and c is the speed of light given as 2.998×10^{8} $m.s^{-1}$

The spectrum of extraterrestrial radiation corresponds approximately to the emission of a black body raised to 5800 K. A standard curve, compiled according to data collected by satellites, is designated as AM0. Its energy distribution is distributed as follows [4]:

Ultraviolet (UV) $0.20 < \lambda < 0.38$ μm => 6.4%

Visible $0.38 < \lambda < 0.78$ μm => 48.0%

Infrared (IR) $0.78 < \lambda < 10$ μm => 45.6%

The following figure illustrates the different solar irradiances.

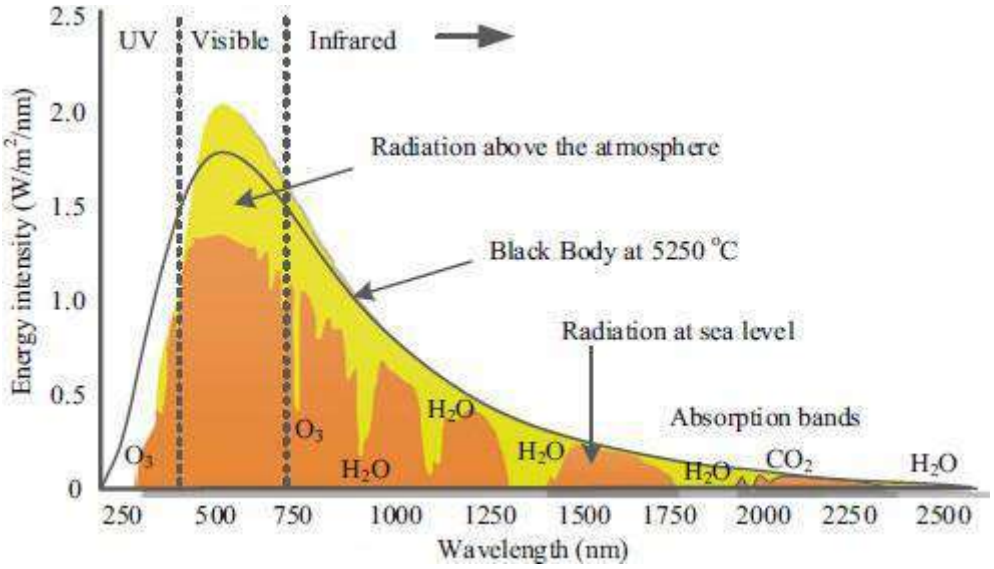

Figure I. 1: At the outer earth's atmosphere (black body), at the top of the atmosphere (AM0) and at the sea level (AM1.5) [5]

From Figure I.1 and Figure I.2, we see that solar radiation can be reflected, scattered or absorbed. On the earth surface, the solar spectrum is not the same as in space, because it is influenced by the absorption of molecules in the atmosphere (O_3, CO_3, H_2O). The climatic conditions as well as the presence of particles also influence the real value of the spectrum. To consider these differences, compare the performance of solar cells and qualify the different solar spectra used, we introduce a coefficient called air mass (AMx) whose expression is [6]:

$$x = \frac{1}{\cos\theta} \qquad \text{(I.2)}$$

Where: θ is the angle between the zenith and the direction of solar radiation.

AM0: Corresponds to conditions outside the atmosphere, such that the power density is 1367 W/m^2.

AM1.5: Corresponds to standard conditions (T = 25°C), such that the power density is 1000 W/m^2.

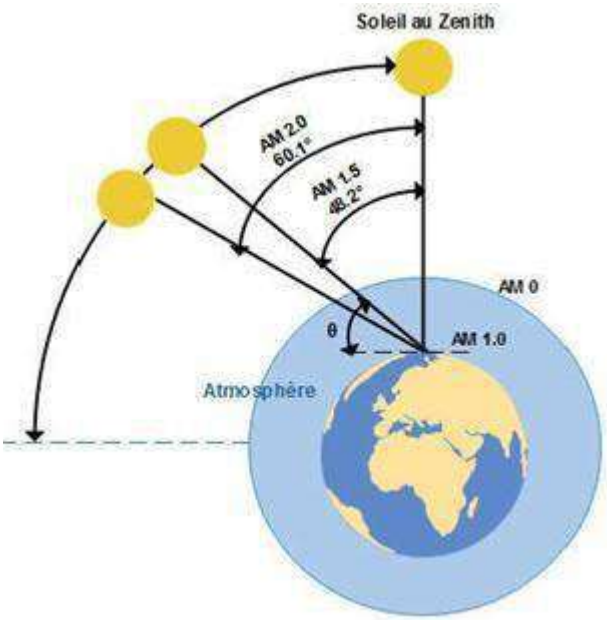

Figure I. 2: Descriptive diagram of the solar incidence on the earth

I. 4. Photovoltaic Solar Cell

I. 4. 1. What is a photovoltaic cell?

A photovoltaic cell is an electronic component based on semiconductor materials. Its operation depends on the exposure of light to generate an electrical voltage (the photovoltaic effect) of approximately 0.5 V with a direct current.

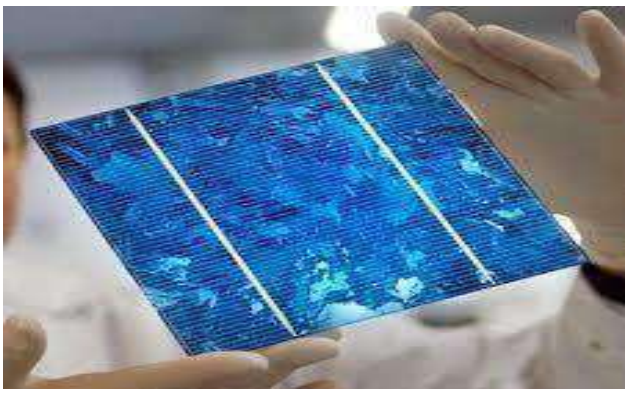

Figure I.3: Photovoltaic solar cell [7]

I. 4. 2. Operating principle of a photovoltaic solar cell

The PV solar cell is a semiconductor component converting incident illumination into electrical power [1], this phenomenon called the photovoltaic effect, which consists of the appearance of a potential difference produced by the generation of charge carriers by light excitation at the vicinity of a PN junction; the following steps explain this conversion phenomenon (See Figure I. 4):

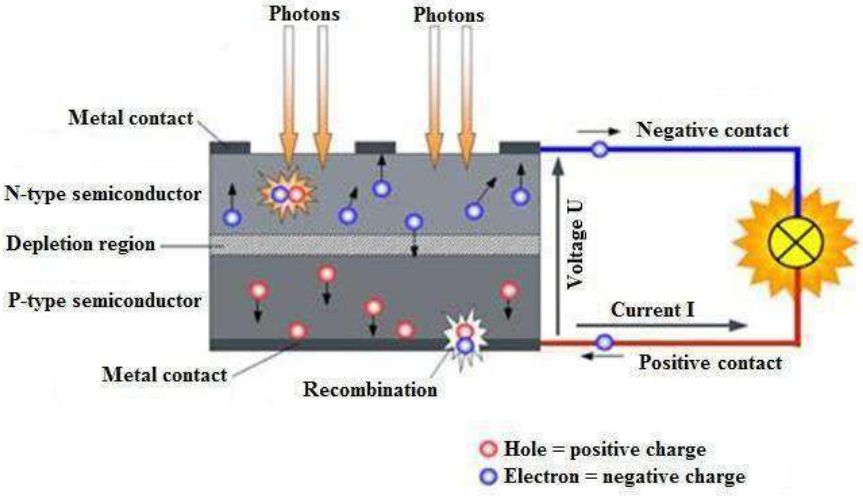

Figure I. 4: Movement of free charge carriers in a solar cell based on a single PN junction

1)- Absorption of photons (whose energy is greater than the gap) by the material constituting the device;
2)- Conversion of photon energy into electrical energy, which corresponds to the creation of electron-hole pairs in the semiconductor material;
3)- Collection of particles generated in the device [4].

I. 4. 3. Ideal solar cell

If the characteristic of the junction is of the form:

$$I_d = I_s\left(e^{\frac{qV}{nKT}} - 1\right) \quad \text{(I.3)}$$

We can admit that in the presence of light, there is appearance of an additional photocurrent, I_{ph} whose direction is opposite to the direct current. By connecting an external circuit to the solar cell, this current is collected. The current under light is [2]:

$$I = I_{ph} - I\left(e^{\frac{V}{nU_t}} - 1\right) \quad \text{(I.4)}$$

The voltage V is given by:

$$V = QU_t \ln\left(\frac{I_{ph} + I_s - I}{I_s}\right) \quad \text{(I.5)}$$

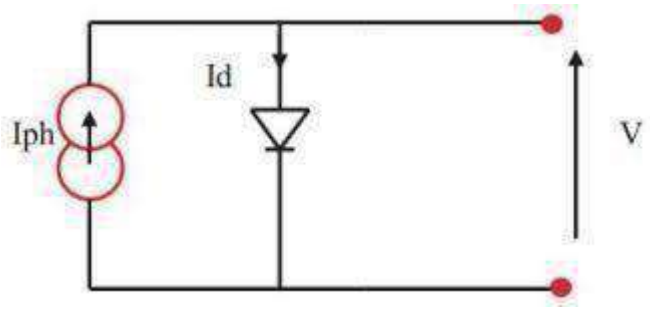

Figure I.5: Equivalent diagram of an ideal photovoltaic cell

I. 4. 4. Real solar cell

Figure I.6 presents the equivalent diagram of a real solar cell, where two parasitic resistances are introduced in this diagram, they will influence the I(V) characteristic of the cell.

The first is series resistance. This resistance is related to the impedance of the electrodes and the base.It follows that the voltage V at the terminals of the cell is different from the voltage at the terminals of the junction.

The second is the shunt resistance, which corresponds to losses in the surface and losses due to defects in the material. As a result, this resistor will divert part of the current and it cannot be delivered to the load.

The equation of the characteristic I(V) of the photovoltaic cell taking into account the resistances and is therefore written [2]:

$$I(V) = I_{ph} - I_d - I_{sh} \quad \text{(I.4)} \qquad \text{(I.6)}$$

$$I(V) = I_{ph} - I_s \left[e^{\frac{V + R_s I}{QU_T}} - 1 \right] - \frac{V + R_s I}{R_{sh}} \qquad \text{(I.7)}$$

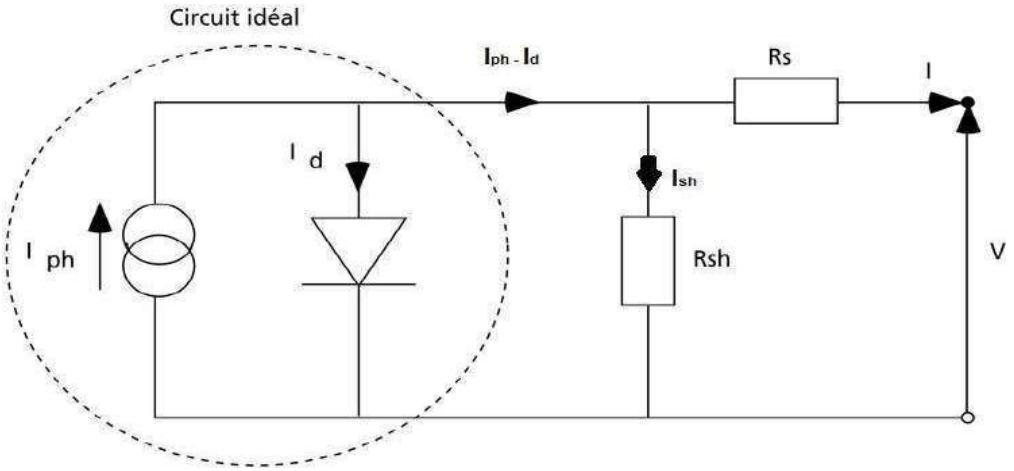

Figure I.6: Equivalent diagram of a real photovoltaic cell

I. 5. Semiconductor materials

Semiconductor materials are used in the majority of electronic systems. They are bodies whose resistivity is intermediate between that of conductors and that of insulators. The conductivity of semiconductors is not as high as that of conductive materials, but they have very useful characteristics.

I. 5. 1. Intrinsic semiconductors

The electrons located on the layer furthest from the nucleus, which participate in the covalent bonds, can under the effect of thermal agitation, become charge carriers.

The energy diagram consists of two bands (conduction and valence) separated by a forbidden band. To cross this band, the electron must acquire energy (thermal, photonic, etc.).

However, the number of free electrons in an intrinsic semiconductor remains very low. Here the number of hole and electron is equal [8].

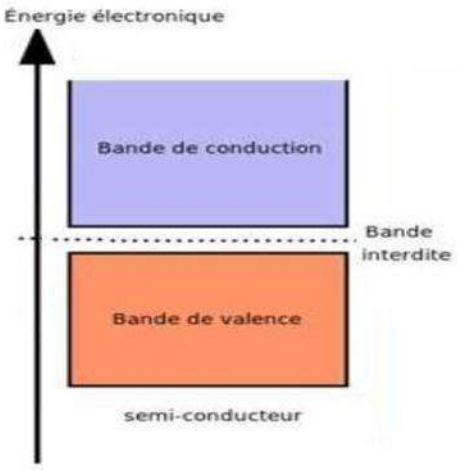

Figure I.7: Band diagram of an intrinsic semiconductor

I. 5. 2. Extrinsic semiconductors

To increase the conductivity of semiconductors, impurities are introduced into them. This process is called doping. The four valence electrons of silicon make it possible to form four covalent bonds with a neighboring atom.

A). P-type doping

We dope the intrinsic crystal with an element having a lower number of valence electrons (on the external layer): we can dope silicon (4 valence electrons) with Boron, Indium, Gallium or Aluminum, which have three valence electrons (acceptor atom). These atoms will take the place of silicon atoms in the crystal. As they have one less valence electron, holes will be created in the semiconductor. The holes become carriers of majority mobile charges: the semiconductor is of the P type. There will remain a few free electrons in the crystal (minority carriers).

The holes thus created will be likely to be blocked by electrons present in the crystal (for example, electrons from electron-hole pairs generated by thermal agitation)

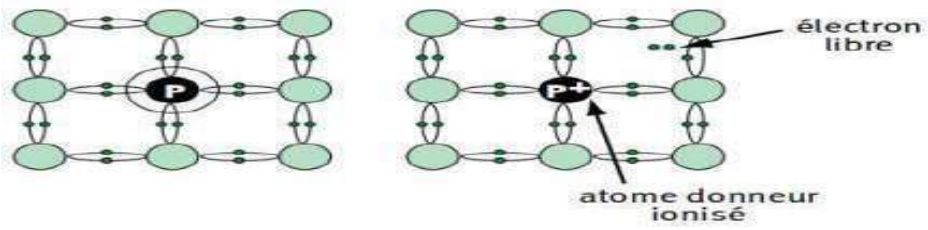

Figure I.8: The four covalent bonds with an acceptor atom

B). N-type doping

The principle is the same as for the P-type semiconductor, except that the crystal is doped with elements having one more valence electron (donor atoms): phosphorus, Arsenic and Antimony, which have 5 valence electrons, can dope silicon for example. Four electrons will make covalent bonds with the surrounding silicon atoms, and the fifth will be a free electron; all these free electrons will be the majority carriers. There will still be some holes, but in very small quantities.

The free electrons will be almost as mobile as in the case of conductors (metallic bonds). In this case, the donor atom becomes a positive ion, but this does not create a hole carrier as in the case of P type silicon, because this positive charge cannot move in the crystal. Note that in both cases (N and P types), the crystal remains globally electrically neutral, because the nucleus of the donor atoms has one more proton than the atom of the intrinsic crystal, and one less in the case of the acceptor atoms. Doping makes it possible to have many more carriers of a given species than of the other, and it has brought an additional fragility in the atomic bonds: the energy necessary to tear a majority carrier from an atom is approximately 0.1eV: there will be more charges participating in the current flow than in an intrinsic crystal.

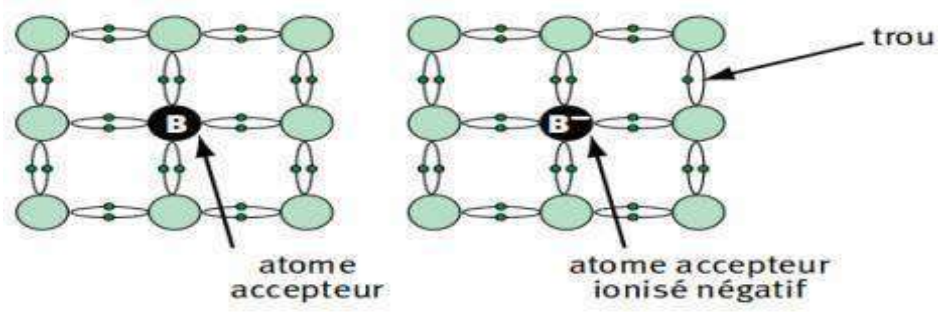

Figure I.9: The four covalent bonds with a donor atom

C). p-n junction (Diode)

One of the key steps in the operation of a PV cell is the separation of electrons and holes before they recombine within the material. This electron/hole separation can be obtained by a potential deference produced by bringing two semiconductors into contact, one p-type and the other n-type, creating a p-n junction.

Under the effect of the concentration gradient, the majority carriers, the holes in the p-type SC and the electrons in the n-type SC will diffuse across the interface, p/n. These

carriers will then recombine. The zone without mobile carrier (ionized atoms) thus created is called space charge zone (ZCE) or depletion zone. There is thus creation of an electric field E that opposes the diffusion of the majority carriers. This electric field allows the migrate on of the holes towards the p-doped zone in the direction of the field and the electrons towards the n-doped zone in the opposite direction to the field [8].

I. 6. Different generations of photovoltaic solar cells

There are three types of solar cell generations:

I. 6. 1. First generation of photovoltaic solar cells (Crystalline silicon form)

The earliest traditional semiconductors (SCs) based on silicon on commercial level are the most efficient SCs at present for daily need and nearly above 80% of all the solar panels spread over the world. Silicon SCs is one of the most efficient systems in terms of single-cell PV modules because of easily available and their abundance on earth surface.

The types of crystalline SCs can be classified based on the type of silicon used and depending on how the Si wafers are made:

- Mono-crystalline (Mono c-Si)
- Polycrystalline (Poly c-Si)

In silicon electronics, a method known as Czochralski method is applied to make wafers of single crystal and is comprised around 30% of the market. Single crystalline silicon is most common and purer than poly c-Si. Poly c-Si is less expensive than single c-Si due to the way of the structural arrangements of silicon.

The largest reported power conversion efficiency for Mono c-Si and poly c-Si solar cell is 26 % and 24 % respectively [9].

I. 6. 2. Second generation of photovoltaic solar cells (Thin films)

The thickness of this type of SCs is found to be thickness of few micrometers. The cost of electricity potentially provided by thin film SCs is lower than that of the c-Si wafer–based SCs of the first generation. Very low thickness is just around 1–4 μm of the thin-film SCs that are consists of successive thin layer of SCs deposited onto a low expansive substrate, viz., polymer, metal, or glass [10]. Secondary SCs based on thin-film SCs are of four primary types as follows that have been developed commercially:

- Copper-Indium-Gallium-Selenide (CIGS)
- Cadmium Telluride (CdTe)
- Amorphous silicon
- kesterites (CZTSSe)

The highest solar cells efficiencies based on CIGS, CdTe, a-Si and CZTSSe are around of 23.35%, 22.1%, 10.2% and 13% respectively [9].

I. 6. 3. Third generation of photovoltaic solar cells

Because of more expensive SCs of first generation and low availability of the materials for the production of the second-generation SCs and their toxicity effect, a third kind of SCs emerged and named as third generation SCs. Third-generation SCs are inherently different from the first and second generations of SCs because it does not depends upon p-n junction design like others. It is based on the development various new materials besides silicon such as silicon wires, nanomaterials, organic dyes, solar inks using conventional printing press technologies, and conductive plastics [11].

Third-generation solar cells can be classified into four types; Dye synthesized solar cells, Organic/Polymer solar cells, Nanostructure Quantum dot solar cells, Perovskite solar cells. Their best efficiencies are 12.25 %, 18.2 %, 18.1 %, and 25.5 % respectively [9].

Figure I-10 shows the evolution of the record efficiencies of the main current photovoltaic sectors [12].

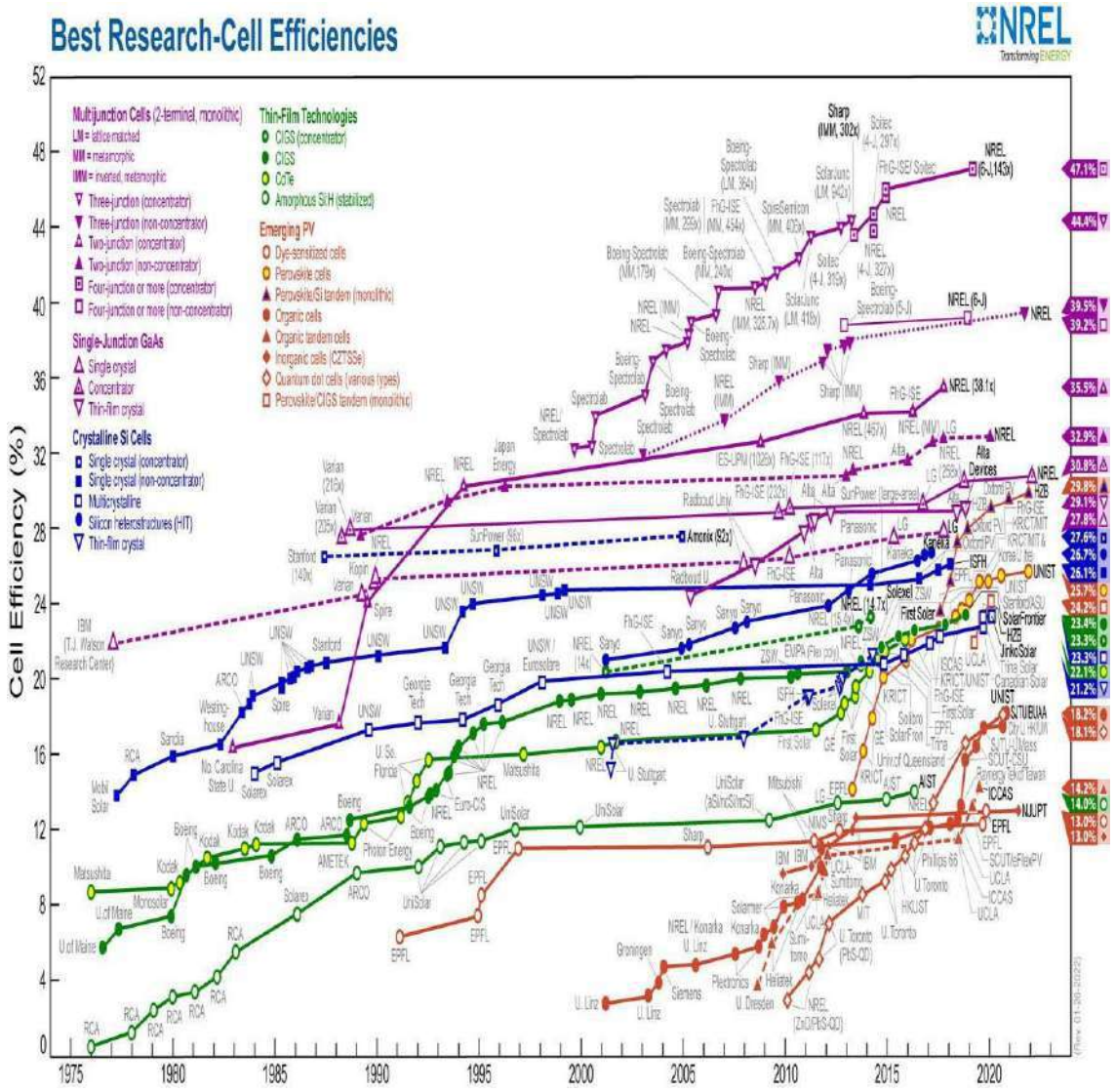

Figure I. 10: Evolution of record efficiency of photovoltaic cells obtained in different laboratories (Source: National Renewable Energy Laboratory (NREL)

I. 7. Advantages and disadvantages of photovoltaic energy

I. 7. 1. Advantages

- ✓ High reliability because the majority of photovoltaic module manufacturers guarantee their products for up to 25 years.
- ✓ The modular option that photovoltaic panels make it easier to adapt the assembly with power applications ranging from milliwatts to megawatts.

- ✓ Reduced operating and maintenance cost.
- ✓ This technology has a positive ecological impact.

I. 7. 2. Disadvantages

- ✓ Manufacturing cost of some photovoltaic sectors remains high because of its investment.
- ✓ Solar installations require enormous surfaces for their operation.
- ✓ The efficiency remains relatively low so far (28% on the market).
- ✓ Weak competition between solar generators compared to diesel or natural gas generators.
- ✓ The most crucial point is the energy storage, which requires batteries, which influences the cost of the installation.

I. 8. Conclusion

This chapter allowed us to become familiar with the photovoltaic field in order to understand the other chapters.

Chapter II

Pbs-based thin-film solar cells

II. 1. Introduction

Lead sulfide (PbS) is one of the most suitable semiconductor materials with a high absorption coefficient. It has the most favorable and highly stable along with low-cost material. Therefore, researchers pay a lot of attention to this material.

In this chapter, we begin with some general concepts on the technology of thin layers and we give the different methods of deposition of thin layers.

II. 2. Thin film solar cells

Thin film cells considered as 2nd generation cells. In general, this type of cell consists of two types which are based on a-Si silicon and also polycrystalline semiconductors like CIGS and CdTe. Today, the various deposition techniques (CVD) offer great flexibility for the manufacture of semiconductors.

The basic requirement is that the thickness of the thin film is greater than the absorption coefficient, so the greatest amount of light can be absorbed because the thin film solar cells made by semiconductor compositions with a direct gap and high absorption [13,14].

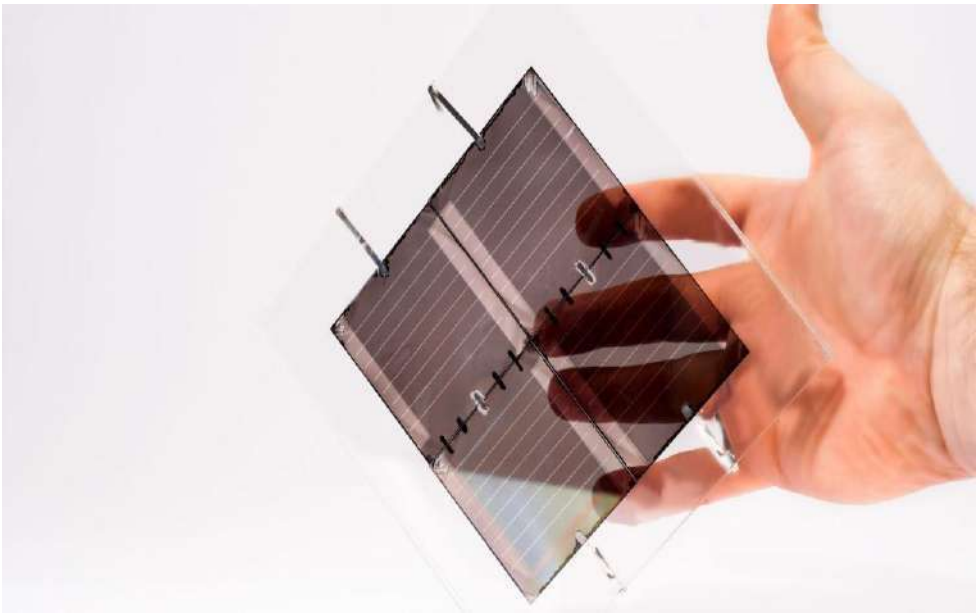

Figure II.1: Thin-film solar cells and modules.

a)-Advantages of thin-type technology

- Low costs as less energy for processing and relatively low material costs are required and large-scale production becomes possible.
- Flexibility in layout techniques that allows the development and use of semiconductors that are difficult to produce.
- It often uses semiconductor materials, which have a direct forbidden band so the absorption coefficient is very high.

b)-Disadvantages

- The difficulty of obtaining different layers that adhere to each other;
- The difficulty of achieving uniformity of thickness, composition and quality across a large substrate;
- The problem of defective interfaces resulting from the mismatch between the meshes of the materials.

II. 3. Thin film characterization technique

The techniques for analyzing and characterizing materials are diversified because the needs of research carried out on the material are also very diverse. We will mention 3 types:

a). Structural characterization

These techniques are based on different types of analysis such as X-ray diffraction, which gives the crystalline structure of the materials, and different types of microscopes such as the atomic force microscope (AFH), Or Raman microscopy that allows obtain additional information on diffraction and infrared spectroscopy techniques.

b). Optical characterization

It consists of two types:

- **Visible Spectroscopy**

  Technique, which is based on the interaction of electromagnetic radiation and matter in the field of near UV a very near I R, this technique makes it possible to find the optical constants of the material studied above all (the rate of transparency, the absorption coefficient, the gap optics and the extinction coefficient).

- **Ellipsometry**

  The measurement of the thicknesses and indices of thin layers is called ellipsometry. There are several types of ellipsometry based on the same operating principle, but the most used are:

  - Extinction Ellipsometer
  - Ellipsometer with phase modulation
  - Ellipsometer with rotating element.

c) Electrical characterization

Mention may in particular be made of the current-voltage I(V), Capacitance-voltage C(V) characteristics for determining the density of oddities, the four-point method (measurement of resistance), the Hall effect for measuring the mobility of charge carriers.

II. 4. Thin Film Deposition

Thin film deposition is the process of creating and depositing thin film coatings onto a substrate material. These coatings can be made of many different materials, from metals to oxides to compounds. Thin film coatings also have many different characteristics which are leveraged to alter or improve some element of the substrate performance. For example, some are transparent; some are very durable and scratch-resistant; and some increase or decrease the conductivity of electricity or transmission of signals.

Thin film deposition is an important manufacturing step in the production of many opto-electronic, solid state and medical devices and products, including consumer electronics, semiconductor lasers, fiber lasers, LED displays, optical filters, compound semiconductors, precision optics, microscopy & microanalysis sample slides, and medical implants. There are a few different technologies and methods that can be used to apply thin film coatings, and an array of tools and equipment that can be used to streamline or enhance the thin film deposition process.

There is no one-size-fits-all, perfect thin film deposition system or method. Your technique and configuration of choice depends on the performance and production requirements that are unique to your application.

II. 4. 1. Physical methods

a. EVAPORATION

There are multiple types of evaporative deposition:

• E-beam evaporation (electron beam): In this process, a highly-charged electron beam evaporates the target material. The evaporated material is then deposited onto the substrate,

and the atoms formed create the thin film. This process is often used for optical thin films such as solar panels, glasses and architectural glass.

• Ion assisted deposition (IAD): This process produces films with less scatter than typical evaporation.

• Thermal evaporation: In this simpler form of PVD, a resistive heat source heats the target material until vapor pressure is produced. The evaporated material then coats the substrate, forming the thin film. It is used to deposit metals such as silver and aluminum for OLEDS, solar cells and thin film transistors [15].

b. MAGNETRON SPUTTERING

Magnetron sputtering is a versatile, plasma-based coating technique. In this process, magnetically confined plasma is created near the surface of the target material. Ions from that plasma collide with the target material, and the atoms ejected from those collisions are what are "sputtered", or deposited onto the substrate to create the thin film. It is often used for metallic or insulating coatings for optical and electrical purposes [15].

c. ION BEAM SPUTTERING

Ion beam sputtering (IBS) is also called ion beam deposition (IBD). This process uses an ion source to sputter the target material—either metallic or dielectric—onto the substrate, forming the thin film. Thin films created through ion beam sputtering are of a high quality, and have very precise thickness due to the monoenergetic ion beam used. This process is often used to create coatings for precision optics and semiconductors, where the utmost precision is required.

d. PULSED LASER DEPOSITION (PLD)

Pulsed laser deposition is a type of evaporation process that uses laser pulses to evaporate the target material. This produces a plume of plasma that then deposits onto the substrate, forming the thin film. While optimizing this process can require more time and effort than other methods, due to the many variables at play, its benefits include high deposition rates and a streamlined process, as well as no filaments for easier maintenance [15].

II. 4. 2. Chemical methods

a. ATMOSPHERIC PRESSURE CVD

In this process, which takes place at normal, or atmospheric, pressure and a lower temperature than other methods, the substrate is exposed to at least one volatile precursor. The precursor(s) react on the surface of the substrate to deposit the thin film. It can be used to deposit doped and undoped oxides, and the deposition is fairly quick. Thin films produced by this method are low-density and have moderate coverage.

b. LOW-PRESSURE CVD

In low-pressure CVD, heat is used to break down a precursor gas inside the chamber where the reaction will take place. This causes the reactive gas to react with the substrate when it is injected into the chamber, and this reaction creates the thin film coating. Low-pressure CVD is commonly used for the deposition of materials including polysilicon and silicon nitride, and can be useful for batch processes. Coatings created with this process are more uniform and feature fewer defects, but the process requires a higher temperature, which can limit the materials available to use [15].

c. ULTRAHIGH VACUUM CVD

Ultrahigh vacuum CVD, the substrate is exposed to precursor gases in an ultrahigh vacuum ($<10^{-6}$ Pa). These precursors then react and deposit onto the substrate, forming the thin film.

d. ATOMIC LAYER DEPOSITION

While atomic layer deposition falls under the CVD umbrella, it differs in that precursor materials are kept separate during the reaction. In this process, the reaction occurs due to sequential pulsing of precursor vapors—one atomic layer is formed during each pulse. Pulses are repeated until the thin film reaches its desired thickness. Benefits of atomic layer deposition include high quality defect-free coating, as well as improved thickness uniformity [15].

e. PLASMA-ENHANCED CVD

Plasma-enhanced CVD is a lower-temperature alternative to standard CVD, and is often used in the production of electronic devices. One common application for PE-CVD coatings is to protect these devices from corrosion. It can create, for example, high-quality silicon dioxide (SiO_2) film at 300°C to 350°C as opposed to the temperature range of 650°C to 850°C required by standard CVD to create similar films. In plasma-enhanced CVD, a pair of reactive gases are excited to create a plasma. This causes a chemical reaction that result in the thin film being deposited onto the substrate [15].

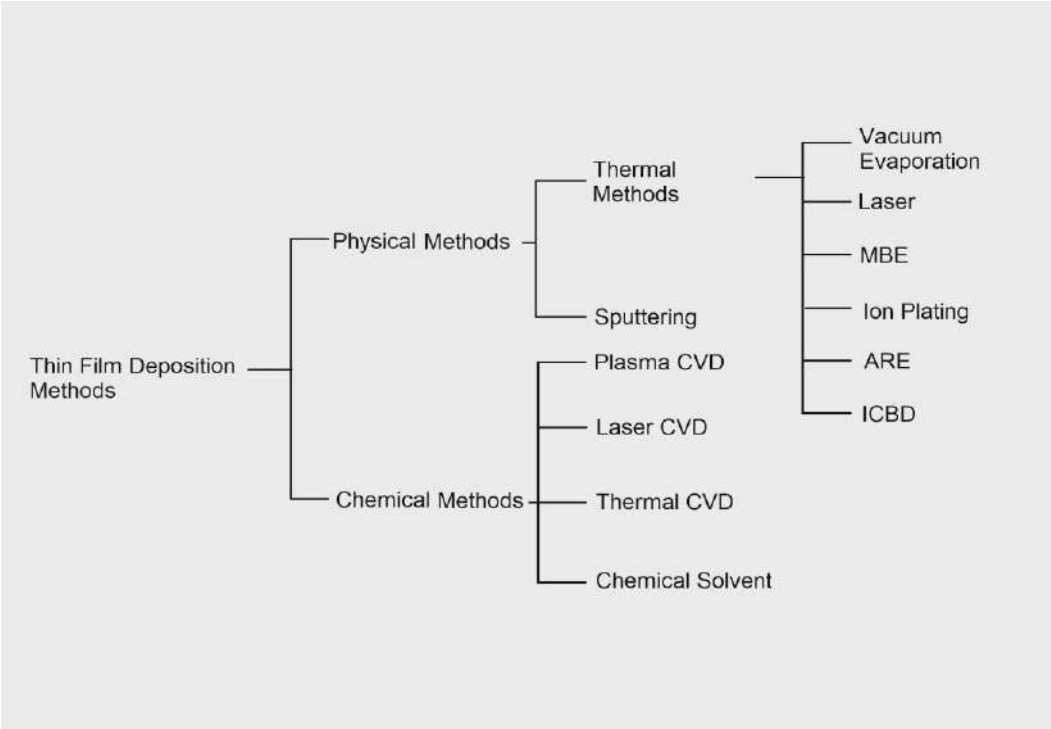

Figure II.2: Schematic classification of the different methods for producing thin layers

II. 5. Thin film layers of lead sulphide (PbS)

Lead sulphide (PbS) is an important direct narrow gap semiconductor material with a band gap of 0.4 eV and has a cubic structure. Due to their suitable bandgaps, PbS thin films are extensively used in IR detectors [16].

Thin film of lead sulphide was established to have very significant application in the manufacture of photoconductive infrared detectors, transistors, contact rectifiers, prisons, lenses, windows and other components of optical system [17]. This material has also been used in many fields such as humidity, photography, solar absorption photoresistance, diode lasers, and temperature sensors, decorative and solar control coatings [18-19]. The chemical bath deposition (CBD) method is attracting considerable attention, as it does not require sophisticated instrumentation. It is relatively cheap, simple to handle, convenient for large area deposition and capable of yielding good quality thin films..

II. 8. Conclusion

In this chapter, we made a reminder on the thin layers and the various techniques of deposition and we presented the Pbs material which constitutes the essential part for the photovoltaic cell which we are going to study in what follows as well as the description of a cell based on Pbs.

Chapter III

Simulation of a Pbs-based photovoltaic solar cell

III. 1. Introduction

Modeling of photovoltaic devices, (PV) is an essential tool in order to improve the efficiency of these PV cells and also reduce their manufacturing cost. These models make it possible to better understand the impact of different physical parameters on the performance of these cells. Design and optimize different types of cells without systematically use experimental processes, which can be expensive, assess the potential of a structure and its maximum theoretical efficiency. Several Simulation software for PV devices is currently available, free to access or under license.

In this chapter, we will present the basic modeling equations used by SCAPS software, as well as a brief description of the simulation method by this software. Then, using simulation by SCAPS software, we will study the influence of the thickness, the bandgap, the doping density and the defect density of the absorber layer on the short circuit current (JSC), the open circuit voltage (VCO), the fill factor (FF), and the conversion efficiency (η) of a PV solar cell based on PbS. This has allowed us to deduce optimal values giving the best performance of the cell.

III. 2. Fundamental equations in semiconductors

Semiconductors physics is an area very rich in modeling and mathematics problems. It consists of a fundamental set of equations that bring together electrostatic potential and load carriers in a very specific field of simulation. These equations, which are resolved via specific software for simulating semiconductor-based devices, are derived from Maxwell equations.

They are mainly: Poisson's equation and continuity equations for both electrons and holes given by the following equations, which are used by SCAPS [20]:

$$\frac{\partial^2\Psi}{\partial x^2} + \frac{q}{\epsilon}[p(x) - n(x) + N_D - N_A + \rho_p - \rho_n] = 0 \quad \text{(III.1)}$$

$$\frac{1}{q}\frac{dJ_p}{dx} = G_{op}(x) - R(x) \quad \text{(III.2)}$$

$$\frac{1}{q}\frac{dJ_n}{dx} = -G_{op}(x) + R(x) \quad \text{(III.3)}$$

Where, ε is the dielectric constant, q is the electron charge, N_A and N_D are acceptor and donor type density respectively, Ψ is the electrostatic potential, p, n, ρ_p , ρ_n, J_p, J_n are hole concentration, electron concentration, hole distribution, electron distribution, current densities of hole and current densities of electron respectively. Gop is the optical generation rate, R is the net recombination from direct and indirect recombination. All of these parameters are the function of the position coordinate x.

III. 3. Presentation of the software used

SCAPS (a Solar Cell Capacitance Simulator) is a one-dimensional solar cell simulation program developed at the Department of Electronics and Information Systems (ELIS) of Ghent University, Belgium. Several researchers have contributed to its development: Alex Niemegeers, Marc Burgelman, Koen Decock, Stefaan Degrave, Johan Verschraegen.

The program was originally developed for cell structures of the $CuInSe_2$ and CdTe family. An overview of its main features is given below [21]:

• Up to 7 semiconductor layers;

• Almost all parameters can be graded (ie based on composition or cell depth). ex: χ, ε, Nv, $vth\ n$, μn, μp, Na, Nd, all traps (defaults Nt);

• Recombination mechanisms: band to band (direct), Auger, SRH type;

• Defect levels: in bulk or at the interface; their state of charge and recombination are taken into account;

• Defect levels, charge type: no charge (idealization), monovalent (single donor, acceptor), divalent (dual donor, dual acceptor, amphoteric), multivalent (user defined);

• Defect levels, energy distributions: single level, uniform, Gauss, tail or combinations;

• Defect levels, optical property: direct excitation with light possible (photovoltaic effect impurity, IPV);

• Metastable defects: transitions between the acceptor and donor configurations for metastable defects known in CIGS: the V_Se defect and the In_Cu defect; also implemented custom metastable transitions;

• Contacts: working function or flat band; optical property filter (transmission filter reflection);

• Tunneling: intra-band tunneling (within a conduction band or within a valence band); tunneling to and from interface states;

• Generation: either from the internal calculation, or from the G(x) file provided by the user;

• Lighting: a variety of standard and other spectra included (AM0, AM1.5D, AM1.5G, AM1.5G edition2, monochromatic, white,);

• Lighting: either on the p side or on the n side; spectrum cut and attenuation;

• Working point for calculations: voltage, frequency, temperature;

• The program calculates energy bands, concentrations and currents at a given operating point, J-V characteristics, ac characteristics (C and G as a function of V and/or f), and spectral response (also with light polarization or voltage);

• Batch calculations possible; presentation of results and settings based on batch parameters;

• Loading and saving of all parameters; start SCAPS in a custom configuration; a scripting language including a free user function;

• Very intuitive user interface;

• A scripting language function to run SCAPS from a "script file"; all internal variables are accessible and traced via the script;

• A built-in curve fitting function;

• A panel for the interpretation of admittance measurements;

• The ordering of all parameters can be defined from a file; more analytical “ranking laws” implemented;

• New analytical models for spectrum, generation and optical absorption coefficient.

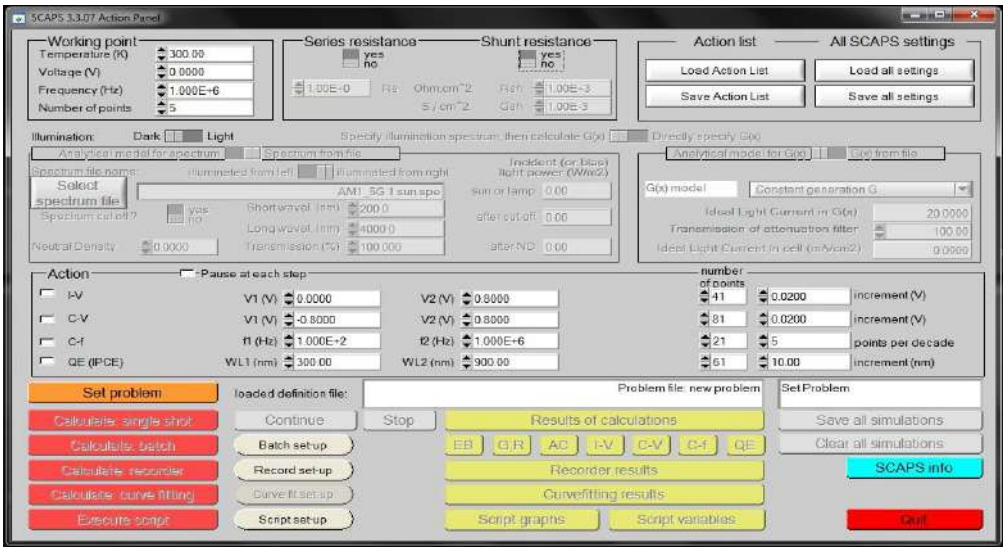

Figure III.1: SCAPS software interface (main window)

III. 4. Presentation of the studied solar cell

The structure to be studied is a heterojunction cell, the basic diagram of which is represented in figure III.2. It consists mainly of the following semiconductor layers: ZnO (TCO window), CdS (buffer) and PbS (absorber).

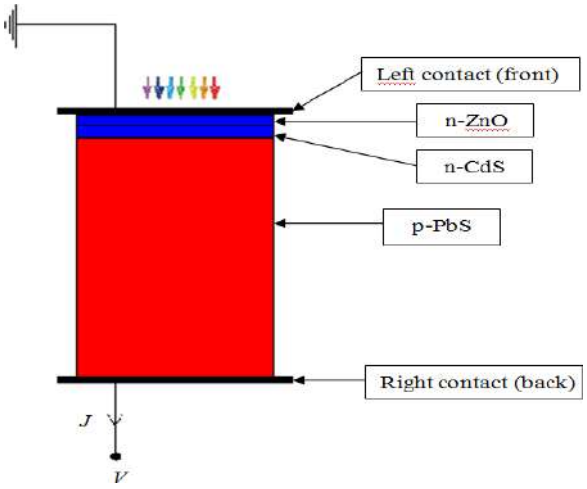

Figure III.2: structure of the studied cell

- **Substrate**

  Generally, the PbS/CdS cell consists of a glass substrate;

- **TCO layer (Transparent Conducting Oxide)**

  It is a layer, which constitutes the front face contact, which must be transparent, anti-reflective and conductive. In this layer, different materials such as ZnO are used. Conductive transparent oxides are large gap materials;

- **Buffer layer of CdS**

  This material is most used as a window thanks to their good electronic affinity and a transparent layer of n-type CdS is deposited;

- **Absorber layer**

  It is a layer with a large optical absorption coefficient $>10^5$ cm^{-1} in the visible and at a very high carrier mobility, the PbS layer is deposited on the CdS layer, the PbS layer must be thin, 5 µm of possible thickness and this layer can be deposited on different due to its high plasticity, these layers have good mechanical strength;

- **Rear face contact**

  It is an ohmic and metallic contact of great work to come out, in this layer we use several metals like (Al, Mo, Cu, Au) posed by evaporation on the layer of PbS.

The table (III.1) gathers all the physical parameters of the three layers ZnO, CdS and PbS according to the SCAPS database.

Table III.1: Specific physical constants of Zno, Cds and PbS at 300 K [22].

Material	p-PbS	n-CdS	ZnO
Layer thickness (µm)	**3.00**	**0.05**	**0.2**
Electronic affinity χ (eV)	**4.35**	**4.4**	**4.6**
Relative permittivity, εr	**10**	**10**	**9**
Mobility of electrons µp (cm2.V-1.s-1)	**25**	**100**	**100**
Hole mobility µn (cm2.V-1.s-1)	**100**	**25**	**25**
Concentration of acceptor atoms, NA (cm–3)	**$5.5*10^{16}$**	**-**	**-**
Concentration of donor atoms, ND (cm–3)	**-**	**10^{17}**	**10^{21}**
Gap energy, Eg (eV)	**1.4**	**2.4**	**3.4**
Density, CN (cm–3)	**$2×10^{18}$**	**$2.24×10^{18}$**	**$2.2×10^{18}$**
Density, NV (cm–3)	**$2×10^{18}$**	**$1.8×10^{19}$**	**$1.8×10^{19}$**
Thermal velocity of electrons, (cm/s)	**10^{7}**	**-**	**-**
Hole thermal velocity, (cm/s	**-**	**10^{7}**	**10^{7}**

Tables (III.2) and (III.3) represent some parameters used for SCAPS-1D simulations.

Table III.2: Material defect levels [22].

Materials	ZnO	CdS	PbS
Type of load	Neutral	Neutral	Neutral
Density (cm-3)	10^{16}	10^{16}	10^{14}
Energy levels (eV, above EV)	0.6	0.7	0.8
Electro capture cross section (cm2)	10^{-15}	10^{-15}	10^{-14}
Effective area of hole capture (cm2)	$5×10^{-13}$	$5×10^{-13}$	10^{-14}

Table III.3: Interface defect Parameter [22]

PbS/CdS interface defect	
Fault type	Neutral
Electron capture cross section (cm-3)	10^{-19}
Hole capture cross section (cm-3)	10^{-19}
Energy distribution	Single
Reference for the fault energy level Et	Above EV
Energy relative to reference (eV)	0.6
Total density (integrated on all energies)	$2*10^{14}$

Our work consists of optimizing by simulation some physical and geometrical parameters of the PbS absorber layer of thin solar cell in order to design a cell with maximum electrical conversion efficiency.

The table (III.4) gathers respectively the technological parameters to be optimized such as the thickness, the doping density and the defect density of the absorber layer in PbS .

Table III.4: Variation range and default values of the optimized parameters of the absorber layer.

Technological parameters	Default values	Variation range
absorber thickness of XPbS (µm)	3.00	0.50 - 5.00
Bandgap (eV)	1.4	1 – 1.7
Doping density (cm^{-3})	5.5×10^{16}	10^{12} - 10^{18}
Defect density (cm^{-3})	5.5×10^{16}	10^{10} - 10^{16}

► In our study, the I(V) characteristics are simulated under AM1.5G solar irradiance conditions for an incident power of 1000 W/m^2.

III. 5. Results and discussions

The difficulty in simulating electronic devices lies in the choice of simulation parameters. In what follows, we are interested in the photoelectric conversion in PbS-based solar cells. the optimization of the output quantities (short-circuit current, open-circuit voltage, fill factor and electrical conversion efficiency) will be done according to the technological parameters concerning the front and base regions in the N^+P junctions, in particular the thickness, the gap, the doping density, and defect density .

III. 5. 1. Effect of the absorber layer thickness

The effect of varying the thickness of the PbS absorber from 0.1 to 3 µm on the I-V characteristic is shown in the following table and figure.

Table III.5: I(V) Characteristics of the cell for different PbS layer thicknesses.

Layer Thickness XPbS (µm)	Voc (V)	Jsc (mA/cm^2)	FF (%)	η (%)
0.10	0.9081	14.07	73.63	9.41
0.20	0.9410	19.12	74.03	13.33
0.30	0.9555	21.72	76.30	15.84
0.40	0.9642	23.50	77.85	17.64
0.50	0.9705	24.80	78.78	18.96
0.6	0.9749	25.78	79.53	19.99
0.7	0.9784	26.55	80.07	20.80
0.8	0.9812	27.16	80.46	21.45
0.9	0.9836	27.66	80.97	21.97
1	0.9856	28.07	80.98	22.41
1.1	0.9871	28.42	81.17	22.78
1.2	0.9885	28.72	81.32	23.09
1.3	0.9896	28.97	81.45	23.36
1.4	0.9906	29.19	81.55	23.59
1.5	0.9916	29.39	81.67	23.80
1.6	0.9923	29.55	81.76	23.98
1.7	0.9931	29.70	81.84	24.14
1.8	0.9937	29.84	81.91	24.29
1.9	0.9943	29.96	81.97	24.42
2	0.9948	30.06	82.03	24.54
2.2	0.9957	30.24	82.11	24.73
2.4	0.9964	30.40	82.18	24.90
2.6	0.9970	30.52	82.24	25.03
2.8	0.9975	30.62	82.28	25.14
3	0.9979	30.71	82.32	25.23

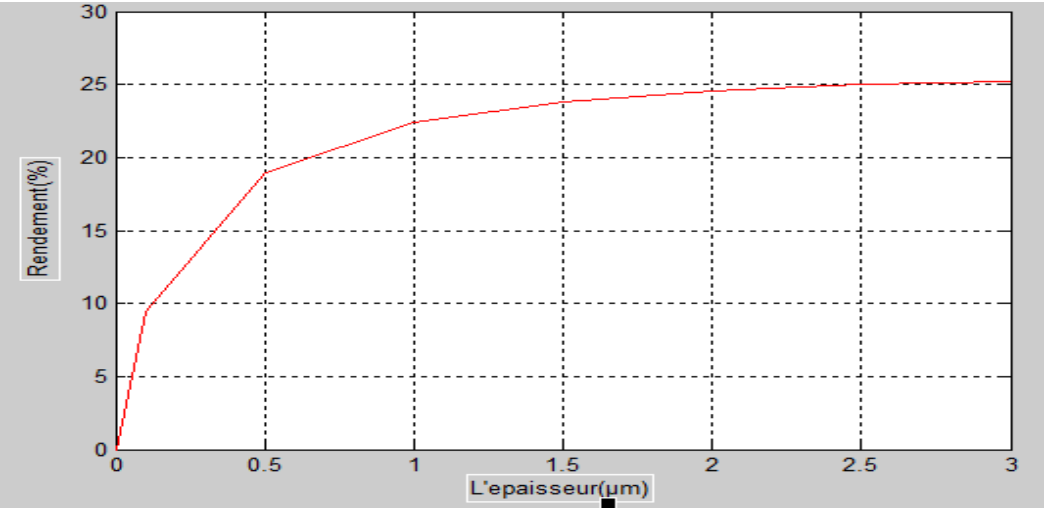

Figure III.3: Effect of the absorber layer thickness on cell performance.

After the variation of the thickness by increasing the absorbent layer (PbS) up to 3µm, we observe that this curve presents an increasing on the efficiency values of the solar cell.

III. 5. 2. Effect of the absorber layer bandgap

The effect of the PbS base gap variation from 1.00 to 1.700 eV [73] on the I-V characteristic is shown in the following table and figure.

Table III.6: I(V) Characteristics of the cell for different values of the PbS layer bandgap.

PbS bandgap Eg (eV)	Voc (V)	Jsc (mA/cm^2)	FF (%)	η (%)
1.000	0.6131	45.91	76.90	21.64
1.100	0.7093	41.60	78.64	23.20
1.200	0.8049	36.92	80.11	23.80
1.300	0.9013	33.68	81.34	24.69
1.400	0.9979	30.71	82.32	25.23
1.500	1.0929	26.84	83.12	24.38
1.600	1.1879	23.58	83.79	23.47
1.700	1.2832	20.81	84.33	22.51

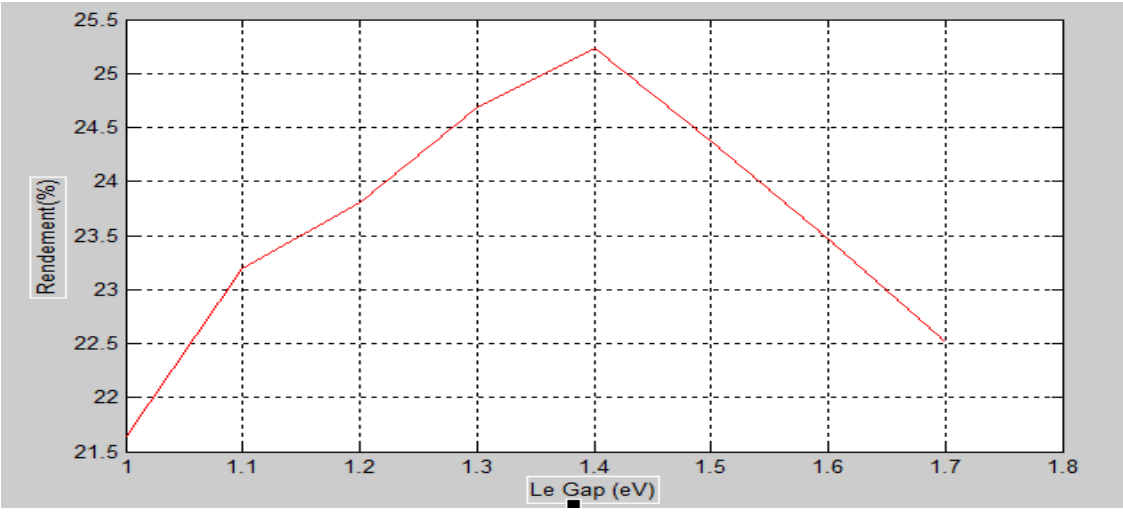

Figure III.4: Effect of the absorber layer bandgap on cell performance.

We also notice that the efficiency (η) undergoes an increase for a gap between 1 and 1.4 eV but begins to decrease when we increase the gap beyond 1.4 eV. The highest efficiency is obtained at the bandgap value of 1.4 eV.

III. 5. 3. Effect of doping density

The effect of the variation of the PbS absorber layer doping density from 10^{12} to 10^{18} cm^{-3} on the (I-V) characteristic is shown in the following table and figure.

Table III.7: I(V) Characteristics of the cell for different PbS doping density.

Doping density N_A (cm^{-3})	Voc (V)	Jsc (mA/cm^2)	FF (%)	η (%)
10^{12}	0.7728	32.17	76.94	19.13
10^{13}	0.8269	32.18	79.11	21.05
10^{14}	0.9756	32.18	82.95	23.37
10^{15}	0.9300	31.95	84.35	25.06
10^{16}	0.9867	31.40	84.25	25.10
$5.5*10^{16}$	0.9979	30.67	82.31	25.23
10^{17}	0.9795	30.46	79.19	23.63
10^{18}	1.0854	29.79	87.34	28.24

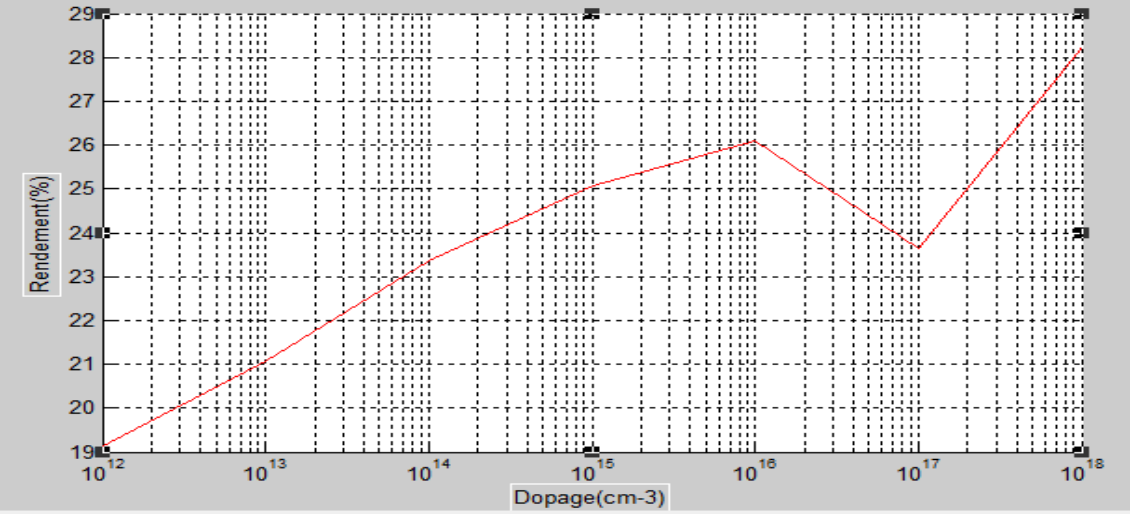

Figure III.5 : Effect of the absorber layer doping density on cell performance.

We notice that the efficiency (η) of the solar cell is increasing with the increase of the doping density up to the optimal value. But after that there is a small efficiency drop to the value of 10^{16} and then it grows.

III. 5. 4. Effect of defect density

The effect of varying the defect density of the PbS buffer layer from 10^{10} to 10^{16} cm^{-3} on the I-V characteristic is shown in the following table and figure.

Tableau III.8 : I(V) characteristics of the cell for different defect density of the PbS layer.

Influence de defect Nt(cm-3)	Tension en circuit ouvert Voc (V)	Courant de court-circuit Jsc (mA/cm2)	Facteur de forme FF (%)	Rendement η (%)
10^{10}	0.9979	31.58	85.70	27.01
10^{11}	0.9979	31.58	85.70	27.01
10^{12}	0.9978	31.58	85.67	26.99
10^{13}	0.9965	31.56	85.55	26.91
10^{14}	0.9867	31.40	84.25	26.10
10^{15}	0.9469	30.49	79.29	22.89
10^{16}	0.8650	28.53	72.37	17.86

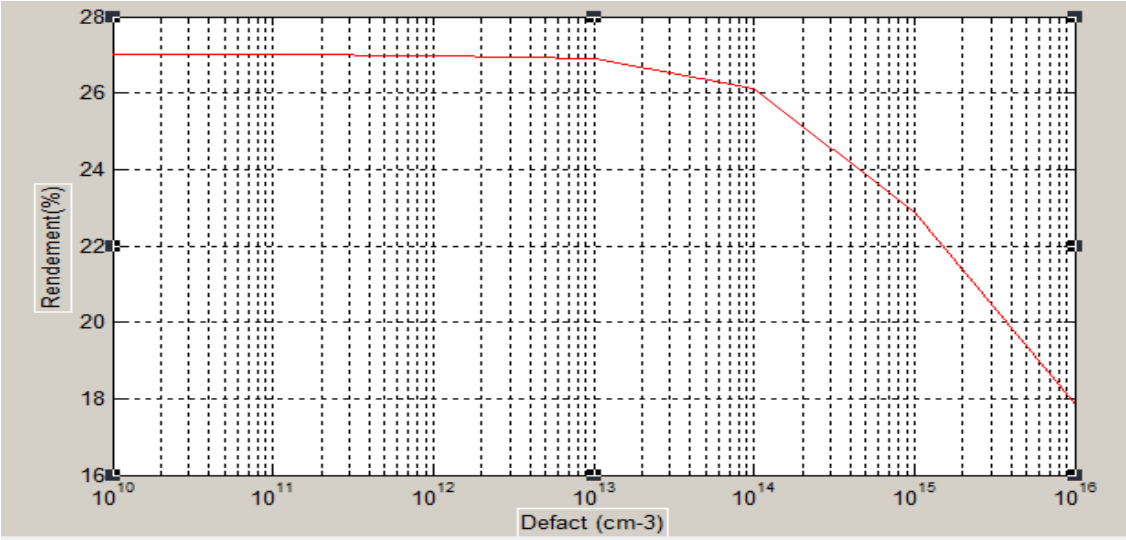

Figure III.6 : Effect of the absorber layer defect density.

We note that the output parameters Jcc, Vco, FF and η of the solar cell decrease as the defect density increases. We obtained a maximum efficiency of 27.01% with a defect density of 10^{10} cm^{-3}. The efficiency decreases as the defect density of PbS increases. Therefore, the probability of recombination of the generated carriers is greater the lower the defect.

III. 6. Conclusion

In this chapter, we used the SCAPS-1D software to optimize some parameters of the PbS absorber layer of a thin film solar cell. The analysis of all of our results shows that the best photovoltaic characteristics for the PbS-based solar cell (V_{CO} = 0.9979 V, J_{sc} = 31.58 mA/cm^2, FF = 85.70 %, and η = 27.01%) are obtained for XPbs = 3 µm, Eg = 1.4 eV, $N_A = 10^{16}$ cm^{-3} and $N_t = 10^{10}$ cm^{-3}.

General conclusion

Chapter I: Basic notions on Photovoltaic Solar Cells

In this work, we relied on the most suitable software for the photovoltaic conversion of semiconductor devices called SCAPS-1D. In this part we have simulated the I(V) characteristic of the PbS-based solar cell under the AM1.5 conditions of solar illumination and we have deduced the output parameters such as: the open circuit voltage (V_{OC}), the short-circuit current (J_{SC}), the fill factor FF and the electrical conversion efficiency (η).

This simulation allowed us to better understand the sensitivity and variation of these quantities as a function of the thicknesses, the bandgap and the doping density of the absorber layer in PbS as well as its defect density.

The analysis of all of our results shows that the best photovoltaic characteristics for the PbS-based solar cell are obtained: V_{CO} = 0.9979 V, J_{sc} = 31.58 mA/cm^2, FF = 85.70 %, and η = 27.01% for XPbs = 3 µm, Eg = 1.4 eV, $N_A = 10^{16}$ cm^{-3} and $N_t = 10^{10}$ cm^{-3}.

Bibliography

Chapter I: Basic notions on Photovoltaic Solar Cells

[1] J. Metzdorf, S. Winter, and T. Wittchen, "Radiometry in photovoltaics: calibration of reference solar cells and evaluation of reference values," Metrologia, vol. 37, no.5, p.573, 2000.

[2] https://fr.wikipedia.org/wiki/Raies_de_Fraunhofer.

[3] P. Lyons, J. Wong, and M. Bhandari, "A comparison of window modeling methods in EnergyPlus 4.0," Proc. SimBuild, vol. 4, no. 1, p. 177–184, 2010.

[4] "American Society for Testing and Materials (ASTM), G173-03, ISO 9845-1 (1992). Available:https://fr.search.yahoo.com/search?fr=mcafee&type=E210FR91105G0&p=American+Society+for+Testing+and+Materials+(ASTM)%2C+G17303%2C+ISO+98451+(1992).

[5] R. J. Komp, "Practical Photovoltaics," Ann ArborAatec Publ., 1995.

[6] S. Fonash, Solar cell device physics. Elsevier, 2012.

[7] H. J. Hovel, "Semiconductorsandsemimetals.Volume11. Solar cells,"1975.

[8] B. O'reganand M. Grätzel, "Alow-cost,high efficiency solar cell based on dye sensitized colloidal TiO2 films,"nature,vol.353,no.6346,p.737,1991.

[9] Green MA, Dunlop ED, Hohl-Ebinger J, Yoshita M, Kopidakis N, Hao X, Solar cell efficiency tables (version 59), Prog. Photovolt Res Appl. 30(1) (2022) 3-12. Doi:10.1002/pip.3506

[10] Ranabhat, K., Patrikeev, L., Revina, A.A., Andrianov, K., Lapshinsky, V., Elena Sofronova, E., An introduction to solar cell technology, J. App. Eng. Science, 14, 405, 2016.

[11] Habisreutinger, S.N., Leijtens, T., Eperon, G.E., Stranks, S.D., Nicholas, R.J., Snaith, H.J., Nano Lett., 14, 5561, 2014.

[12] https://www.nrel.gov/pv/cell-efficiency.html

[13] Thalía Jiménez et al, State of the Art on Sb2(S1-x,Sex)3, Gen. Chem. 2019, 5, 180029.

[14] Fatima HADJHERS, investigation of structural, optical, and electrical properties of TTO films produced by RF sputtering Annealing effect, Master's thesis defended on 02/14/2011.

[15] https://www.dentonvacuum.com/resources/what-is-thin-film-deposition

[16] P. Gadenne, Y. Yagil, G. Deutscher, J. Appl. Phys. 66, 3019 (1989).

[17] E. H. Putley, Materials used in Semiconductor Devices, 2nd Ed., John Wiley and sons Ltd. N.Y, (1967).

[18] P. K. Nair, O. Gomezdaza and M. T. S. Nair, Adv. Mater. Opt. Electr., 1, 139 (1992).

[19] R. K. Joshi, A. Kanjilal and H. K. Sehgal, Appl. Surf. Sci., 221, 43 (2004).

[20] S.M. Sze, Physics of Semiconductor Devices, second ed., John Wiley & Sons Inc, 1981.

[21] SCAPS manual most recent. Download with the most recent version, SCAPS 3.3.10 https://scaps.elis.ugent.be/

[22] Mrinmoy Dey et al, Optimization of Lead Sulfide (PbS) Solar Cell, 2019 International Conference on Electrical, Computer and Communication Engineering (ECCE), 7-9 February, 2019.